Red/Green Tunable-emissive Carbon Nanodots for Smart Visual Precision pH Sensing

Jiang-Lin Zhao,[†] Qing-Ying Luo,[†] Qin Ruan,[†] Kai Chen,[‡] Cui Liu,*[⊥] Carl Redshaw[§] and Zongwen Jin*[†]

[†]Institute of Biomedical & Health Engineering, Shenzhen Institute of Advanced Technology, Chinese Academy of Sciences, 1068 Xueyuan Avenue, Shenzhen 518055, China.

[‡]Jiangsu Collaborative Innovation Center of Atmospheric Environment and Equipment Technology, Jiangsu Key Laboratory of Atmospheric Environment Monitoring and Pollution Control, School of Environmental Science and Engineering, Nanjing University of Information Science & Technology, Nanjing 210044, China

[⊥]Institute of Medical Engineering, Department of Biophysics, School of Basic Medical Sciences, Xi'an Jiaotong University Health Science Center, Xi'an, Shaanxi, 710061, P. R. China

[§]Dept. of Chemistry, University of Hull, Hull HU6 7RX, U.K

KEYWORDS: Carbon nanodots, Precision pH sensor, Tunable fluorescence, Smart material, Information encryption

ABSTRACT: The development of novel carbon nanodots (CDs) with excellent optical properties and promising applications is an attractive but challenging area. Herein, we demonstrate that the fluorescence properties of CDs can be optimized by simple modification of the molecular structure of the carbon source. Significantly, the finally optimized CDs **1** exhibit a rare extremely acidic (pH 1 to 3) sensitivity. A distinguishable red/brown/green fluorescence color change is achieved for visual readout by simple tuning the pH 1/2/3. The distinguishable color change combined with ratiometric fluorescence changes, greatly improve naked eye visual resolution up to 0.2 pH units which is higher than commercial precision pH test trips. Furthermore, a smartphone was employed in a portable, low cost, rapid and precise pH measurement method, which satisfied the requirement of point-of-care testing (POCT). Inspired by the reversible color change of red/brown/green tri-fluorescence on tuning the pH to 1/2/3, a simple yet efficient molecular logic circuit has been designed. Given the unique pH dependent photoluminescence properties, these CDs have been further applied in the anti-counterfeiting and information encryption field, making the "Burn after reading" encryption technology a reality.

INTRODUCTION

pH is one of the most fundamental and widely measured parameters, and plays a key role in chemical analyses, environmental monitoring and biological regulation.[1] Since Böttger first introduced electrometic methods for determining H^+ ion concentration, the pH precision problem has been basically solved by routine pH measurements.[2] Nevertheless, with the development of technology, the need for noninvasive and *in situ* pH tests in biological systems, combined with low cost and high precision requirements means that the development of portable rapid pH tests at POCT (point-of-care testing) presents new challenges. Indeed, the use of conventional pH detection methods are unacceptable in these settings. Visual pH sensors offer an opportunity which can be non-destructive, *in situ*, sensitive, observable by the naked-eye, and allow for on-site detection via color change without the need for other instrumentation.[3] After decades of hard work, there are now numerous visual pH sensors which respond over the mild pH range of 4 to 11.[1,4] However, very few sensors can be applied under extreme pH conditions, which is likely due to the inability of the sensor materials to maintain photochemical stability under strongly acidic and basic environments.[5] This is a commonly encountered problem in fluorescence detection processes.[6] However, there is a great need for rapid and accurate measurements at extreme pH values, examples of which include the monitoring of gastric juice (pH 0.8-1.5),[7] acid rain (pH 1.5– 4.5),[8] intracellular pH of acid-fast microorganisms (*e.g.* acidophiles and Helicobacter pylori) and enteric bacteria (*e.g.* Escherichia coli and Salmonella species).[9] It is the luminescent materials that are the key element for a visual pH sensor, and these dictate the photochemical stability, sensitivity, biocompatibility and the end use.

Carbon nanodots (CDs) are an emerging nanomaterial that have been significantly developed given their facile preparation from an abundant carbon source, their low toxicity and excellent biocompatibility. Moreover, given their solubility in water and facile functionalization and

good photochemical stability, CDs are materials with promising potential applications.[10] Since the first discovery of carbon nanodots by Scrivens *et al.* in 2004,[11] numerous methods for the preparation of CDs have been developed.[10] Much effort has been devoted to further improving the optical properties of CDs, which has included surface passivation, functionalization, and doping with various heteroatoms.[12] However, much less research has focused on the exploration of the relationship between the molecular structure and the final photoluminescence properties of the CDs. Lin *et al*. reported in 2015 the tunable

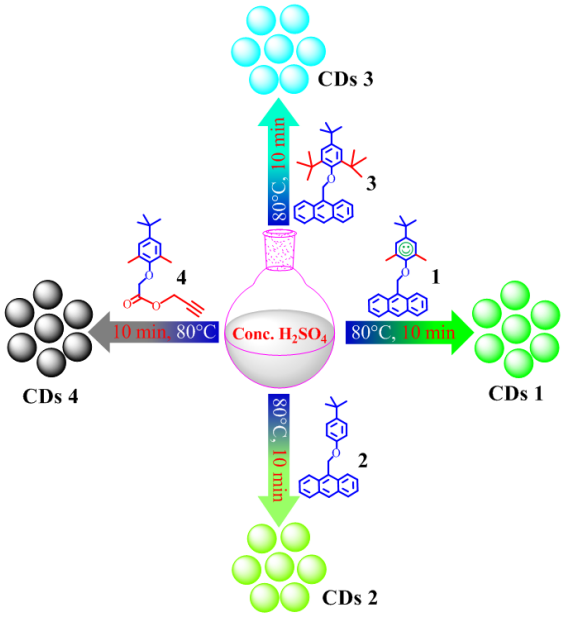

Scheme 1. The schematic of tuning carbon nanodots fluorescence properties by modifying the molecular structure of the carbon sources.

red/green/blue luminescence of CDs with three isomers of phenylenediamine, but highlighted that more in-depth studies were still required to clarify the relationship between the luminescence characteristics and the isomers of the carbon source.[13] More recently, Huang *et al*. indicated that the carbon source is the key when deciding the final structure and optical properties of CDs.[10c] Inspired by the innovated retrosynthesis method to fabricate CD proposed by Li *et al*.,[14] herein a series of anthracene derivatives with a tunable electron donating structure as the carbon source have been studied (Scheme 1).

We have demonstrated that the fluorescence properties of CDs can be optimized by simply modifying the molecular structure of the carbon source. Significantly, the finally optimized CDs **1** exhibited rare extreme acid sensitivity (pH 1 to 3). A distinguishable red/brown/green tri-color change is achieved for visual readout and instrument-free sensing by simply tuning the pH to 1, 2 or 3. Fluorescence titration analysis revealed that CDs **1** exhibited a ratiometric fluorescence change on increasing the pH. Given the distinguishable red/brown/green tri-emission color and ratiometric fluorescence changes, the visual resolution was greatly improved to higher than 0.2 pH units by naked eye observation. Thus, a truly portable precision pH measurement method was realized, akin to a smartphone, which satisfies the needs for application in POCT. Furthermore, the potential application of CDs **1** in a molecular logic circuit "a signal traffic light" and for information encryption is also proposed.

RESULTS AND DISCUSSION

Preparation of CDs. It is well established that it is possible to control the reactive site, reactivity and reaction sequence by the introduction of different functional groups during organic synthesis. Is this strategy also possible for the synthesize of CDs? Herein, 9-((2,4,6-tri-*tert*-butylphenoxy)methyl)anthracene (compound **3**, Scheme 1) was employed as the carbon source. The detailed preparation of the CDs is discussed in the supporting information. In general, after mixing with concentrated H_2SO_4 for 10 minutes, compound **3** would been carbonated affording CDs **3**. The sharp characteristic anthracene moiety absorption band (~350 to 400 nm)[15] of compound **3** was replaced by a weaker wide absorption band from ~320 nm to ~480 nm of the CDs **3** (Figure 1a), which revealed the formation of the various aromatic fused ring structures in the CDs. The gradually decreasing intensity of these aromatic fused rings from 320 nm to 480 nm reflects the fraction of small aromatic fused ring structures present *versus* the larger ones. The obtained CDs **3** exhibited a cyan fluorescence with a 89 nm Stokes shift (λ_{em} = 489 nm, Figure 1b & 1c inset). By simple elimination of the 2,4-bis-*tert*-butyl groups of compound **3**, *i.e*. use of 9-((4-(*tert*-butyl)phenoxy)methyl)anthracene (compound **2**) as the carbon source, it proved possible to red shift the fluorescence of CDs **2** to 516 nm with a weak light yellow green fluorescence (Figure 1b & 1c inset). The Stokes shift increases to 116 nm compared with CDs **3**, and the content of small aromatic fused ring structures in CDs **2** has decreased since the corresponding UV-vis intensity has decreased (Figure 1a). These observations suggested that presence of the *tert*-butyl group affected the carbonation degree and polymerization site during the formation of the CDs. Instrestingly, the fluorescence properties of CDs **2** can be further optimized by the introduction of a methyl group in compound **2**, *viz* 9-((4-(*tert*-butyl)-2,6-dimethylphenoxy)methyl)anthracene (compound **1)**. The

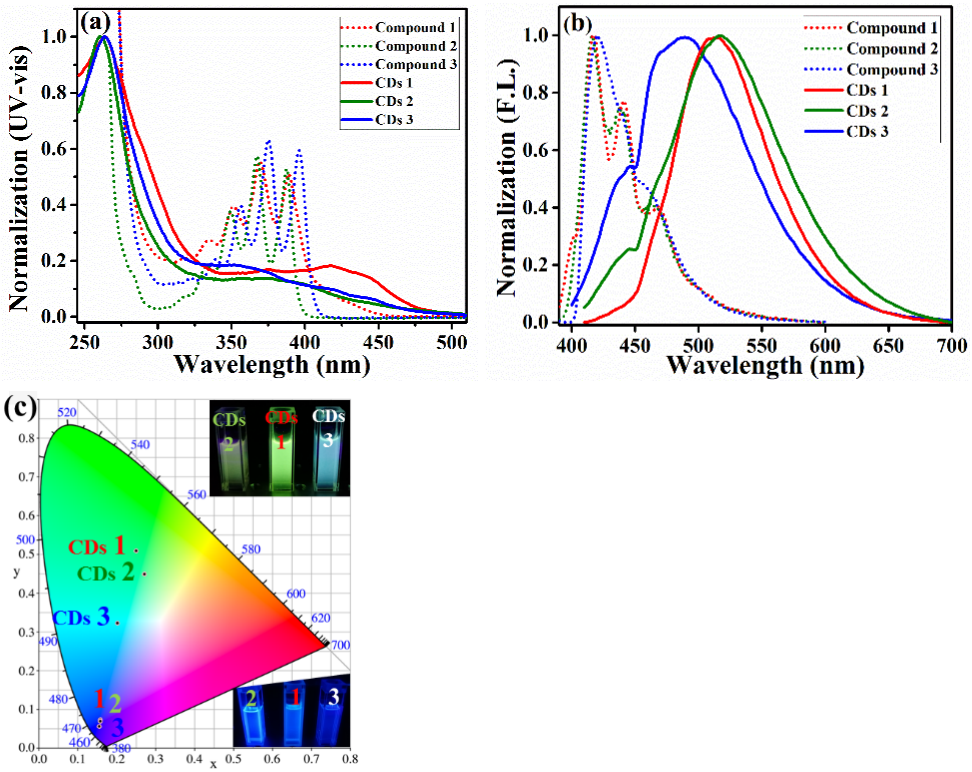

Figure 1. (a) Normalized UV-vis absorption spectra and (b) Normalized fluorescence spectra (λ_{ex} = 400 nm) of compounds **1**, **2** & **3** (carbon source) and the corresponding CDs **1**, **2** & **3**; (c) The 1931 CIE chromaticity coordinate recording the color changes of the above mentioned carbon sources and CDs, where X is the chromaticity coordinate that represents the proportion of red primary and Y is the chromaticity coordinate that represents the proportion of green primary (inset is the photographs of the corresponding solutions under UV light at 365 nm).

introduction of the methyl group resulted in the fluorescence intensity of CDs **1** being greatly increased with a strikingly narrowed peak width; pure green fluorescence was obtained (Figure 1b & 1c inset). This can be ascribed to the increasing content of large aromatic fused ring structures in CDs **1** (Figure 1a). The absolute quantum yield of CDs **1** in water was determined to be 10.1% at 375 nm excitation wavelength using the quantum efficiency measurement system with a calibrated integrating sphere. Given the presence of possible visual errors, we introduced the CIE chromaticity coordinate to accurately record the color changes. As shown in Figure 1c, almost the same photoluminescence for the carbon source of compounds **1**, **2** &**3** was observed, but three different kinds of luminescence CDs were afforded. This can be attributed to the different electron-donating capability of the modified groups affecting the carbonation degree and polymerization site during the formation of the CDs. It is noteworthy that when we used a non-fluorescence compound as the carbon source, such as **4** (a chain hydrocarbon replaces the anthracene group in **1**) (Scheme 1), although we can also obtained water-soluble CDs, the system is almost non-fluorescent suggesting that the anthracene plays an important role in the photoluminescence.

Characterization of CDs. The obtained CDs were fully characterized, and TEM images revealed that the CDs **1** are well dispersed in water (Fig. S2). The size distribution was investigated by choosing about 200 particles randomly, and from the particle size distribution histogram shown in Fig. S2, the CDs **1** size was found to be in the range of 1.9–6.5 nm with an average diameter of 3.9 nm. Similar TEM images have been observed for CDs **2** and CDs **3** (Fig. S3 & S4). ^{1}H NMR spectroscopic analysis revealed that there are three main kinds of proton in the obtained CDs **1**, CDs **2**, and CDs **3**: aromatic protons (broad peak at 6~8 ppm), α-H of hydroxyl or carbonyl (multiple peaks at 3.3~3.7 ppm), and alkane protons (broad peak at 0~1.5 ppm, Fig. S5). However, the distribution of aromatic protons is different among the three CDs, *viz.* the proportion of various fused ring aromatic structures in the CDs is different which is consistent with the UV-vis and fluorescence analysis results (Figure 1). It is strongly suggested that the formation of CDs can be tuned by the introduction of different electron-donating groups in the carbon source. The functional group composition of the CDs sample was further analyzed by FT-IR spectroscopy (Fig. S6). Characteristic absorption bands at 3444 cm^{-1}, 2958/2863 cm^{-1}, 2927 cm^{-1}, 1643 cm^{-1}, 1461 cm^{-1} 1398 cm^{-1}, 1193 cm^{-1}, and 1041 cm^{-1} were assigned to phenol–OH, -CH_3, -CH_2-, Ar-C=C-, C-S, S=O, and C-O stretching vibrations, respectively.[12b,16] The X-ray photoelectron spectra (XPS) of the CDs were recorded to analyze the surface structure and elemental composition of the CDs. The XPS spectra of CDs **1** (Fig. S7a) contained distinct peaks at 285 (C 1s), 532 (O 1s), and another two weak peaks at 168 (S 2p) and 232 eV (S 2s) which indicated that the CDs **1** are mainly composed of C (84.15%), O

(13.12%) and S (2.73%) elements.[17] Fig. S7b shows the high-resolution C 1s spectrum, implying the existence of C=O (287.4 eV), C–O (286.1 eV) and C–C/C=C (284.7 eV). The high-resolution of the O 1s XPS spectrum peaks at 531.9 eV, 533.5 eV, and 534.8 eV revealed the dominant C–O, C=O, and S-O groups (Fig. S7c).[5a,18] In the Raman spectrum (Fig. S8a), the D band at 1363 cm^{-1} is assigned to the disorder or defects in the graphitized structure, and the G band at 1587 cm^{-1} represents the sp^2 carbon networks.[19] The coexistence of D and G bands with an intensity ratio of 0.74 reflects some disorder or defects in the carbon matrix.[19] The XRD pattern (Fig. S8b) exhibits two broad diffraction peaks at 2θ angles of about 23.1° and 42.5°, which are attributable to amorphous carbon composed of aromatic carbon clusters oriented randomly.[19c] The above results are consistent with those of the ^{1}H NMR and FT-IR spectroscopic analyses, indicating that the surface of CDs **1** is rich in carbon-, oxygen- (phenol-OH, CO ether group, and carbonyl) groups as well as some sulfur-containing (SO_3^-) functional groups.

Optical properties of CDs 1. In many previous reports, the fluorescent emission peak of CDs exhibits an excitation-dependent nature.[16] By contrast, no matter which excitation wavelength was selected in the range of 280 to 440 nm, the max emission peak of CDs **1** remained at 514 nm, with only the fluorescence intensity (Fig. S9a) changing. These observations suggested that our obtained CDs possessed predominantly emissive sites with maximum transition probability.[19b]After consideration of the fluorescence intensity and multiple frequency peak effect, 400 nm was selected as the excitation wavelength in this work. Besides, the good anti-photo bleaching property of CDs **1** was observed upon exposure of the CDs **1** under UV-light (365 nm) for 7 h (Fig. S9b).

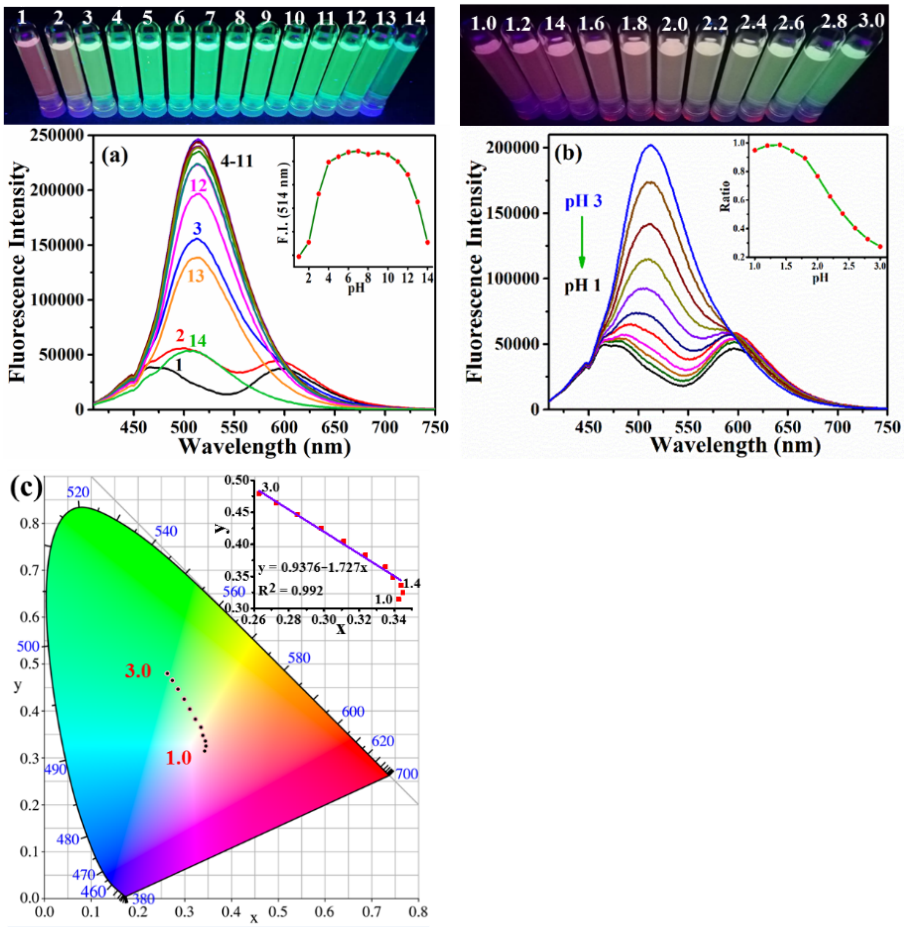

Figure 2. (a) Fluorescence spectra of CDs **1** (5 ppm, λ_{ex} = 400 nm) at different pH values (inset is the fluorescence intensity at 514 nm), photographs showing fluorescence images under UV light of the CDs **1** at pH 1 ~ pH 14. (b) Fluorescence spectra of CDs **1** (5 ppm, λ_{ex} = 400 nm) from pH 1.0 to 3.0 (inset is the ratio of the fluorescence intensity between 596 nm and the max peak (514 nm ~ 466 nm) of the tested pH solution), photographs showing fluorescence images under UV light of the CDs **1** from pH 1.0 to 3.0. (c) The 1931 CIE chromaticity coordinate recorded the color change of the above-mentioned pH (inset is the detail analysis of the color data), where X is the chromaticity coordinate that represents the proportion of red primary and Y is the chromaticity coordinate that represents the proportion of green primary.

Precise pH sensing properties of CDs 1. Interestingly, a unique pH-dependent luminescence phenomenon has been observed in CDs **1**. CDs **1** exhibited an excellent and stable green fluorescence emission over a wide pH range (pH 4 to pH 11) (Figure 2a) and given the good water solubility *in vivo* or *in vitro* studies such as cell imaging (Fig. S10) were possible. Meanwhile, strong acidity (pH < 4) or strong alkalinity

(pH > 11) would result in the fluorescence intensity of the CDs **1** dramatically diminishing. Under strongly acidic conditions (pH 3.0-1.0), a dramatic fluorescence color change was observed as the pH decreased. The original emission peak at 514 nm was split into two main peaks: one underwent a blue shift from 514 nm to ~466 nm with decreasing fluorescence, whilst another was fixed at ~600 nm with almost no change (Figure 2b). This suggested that there were two kinds of emission sites in CD **1**. It is a typical ratiometric change which is considered to be the most accurate fluorescence detection method due to the self-calibration for the environmental disturbance by two-well resolved wavelengths (Figure 2b inset).[18a, 20] On the other hand, UV-vis absorption spectra of CDs **1** under different pH conditions have been carried out (Figure S11). In contrast with the fluorescence spectra, no obvious changes were observed in the UV−vis absorption spectrum of the C-dots as the pH increased from 1 to 14, which demonstrated that there was no ground-state complex formation. This suggested that the H^+ quenches the fluorescence of CDs through a dynamic quenching process.

Previous reports showed that the protonation and deprotonation of functional groups on the surface of CDs could change the energy level, aggregation, and electron/proton transfer, giving rise to the change in the photoluminescence properties.[18b,21] Here, the fluorescence decay curves of CDs **1** at different pH were recorded to further study the possible mechanism of the unique pH-sensitive photoluminescence. For the emission site with a ~500 nm peak which is sensitivity towards pH (ranging from 1.6 to 3.0), the fluorescence lifetime (τ) increased from 2.95 ns (pH 1.6) to 7.54 ns (pH 3.0) as the pH increased from 1.6 to 3.0 (Figure 3a, Table S2). This further suggested that the H^+ quenches the fluorescence of the CDs through a dynamic quenching process. In contrast, for the emission site with a ~600-nm peak which is insensitive towards pH, the fluorescence lifetime was almost constant (9.2-10.0 ns), which indicates that the emission site is related to the internal large conjugated system of the CDs (Figure 3b). Moreover, according to the analysis of the emission ratio, sigmoidal fitting calculated the pKa value to be 2.2, which coincides with the pKa^* of the phenol hydroxyl. The linear range of pH is 1.8-2.8 with R^2 = 0.991. Therefore, the pH-sensitive fluorescence of the CDs may come from the dissociation of phenolic hydroxyl groups on the surface of CDs, which increased the radiation transition rates.[22]

The development of CDs with intrinsic pH-sensitive ratiometric behavior accompanied by significant visual fluorescence changes remains a big challenge.[5a] Herein, the ratiometric change of CDs **1** resulted in colorful changes which can be distinguished by the naked eye (Figure 2b top). The discriminability is up to 0.2 pH units, which is higher than that available to commercial precision pH test trips (*i.e.* Sigma-Aldrich, P3536: pH 6.0-7.7, resolution: 0.3-0.4 pH unit; P4536: pH 4.5-10.0, resolution: 0.5 pH unit) and better than most of the reported resolution for visual precision pH sensors.[1,3,4] A remarkable color change from green (pH 3.0) to pink (pH 1.0) was further recorded by the CIE chromaticity coordinate (Figure 2c). The color change calibration curve exhibited a correlation coefficient as high as 0.992 between pH 1.4 to pH 3.0 (Figure 2c inset). These observations indicated that CDs **1** are capable of being further applied to precise measurements under extreme acidity by the ratiometric fluorescence method and visual colorimetric fluorescence method.

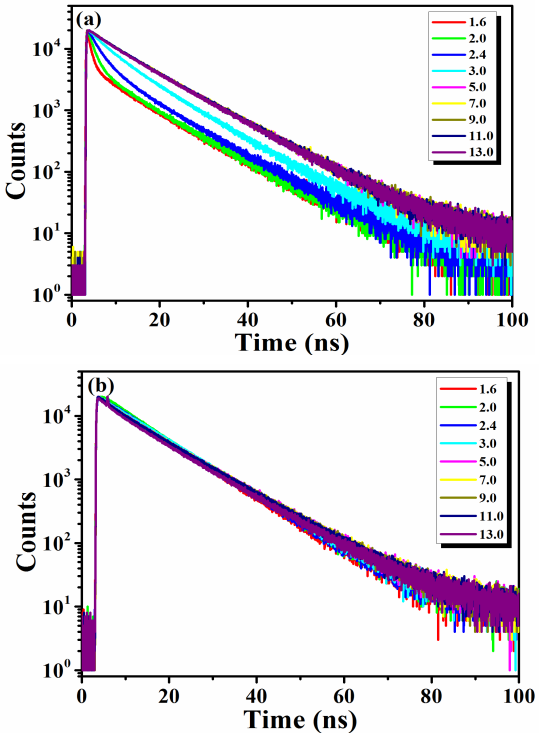

Figure 3. Fluorescence decays for CDs collected at emission maximum for CDs **1** at (a) 500 nm and (b) 600 nm.

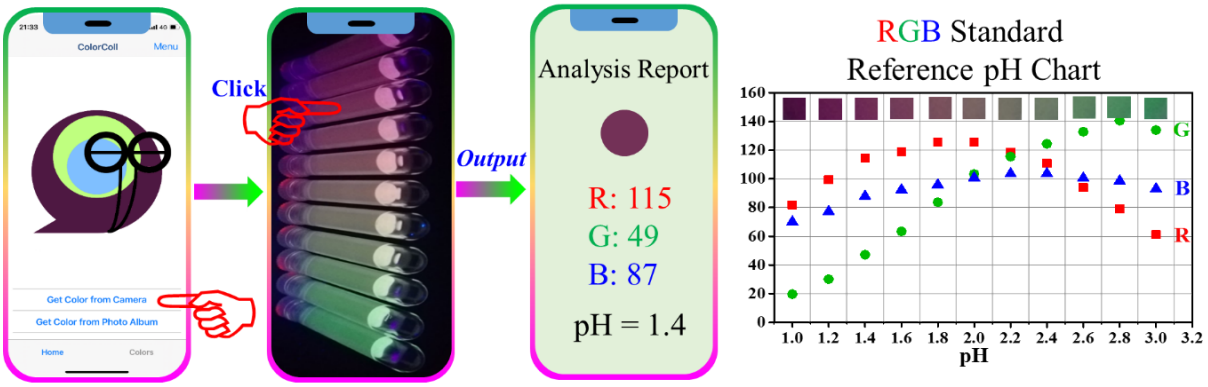

Figure 4. Schematic representation of the smartphone-based pH analysis with on-site monitoring system.

Portable precise pH measurement. Development of emerging technologies, such as smartphone-based sensing technology is likely to lead to the next generation of point-of-care testing devices.[23] Inspired by the colorful changes with the high correlation coefficient for the calibration curve of CDs **1** under extreme acidic conditions, a portable, rapid, precise pH measurement method has been proposed (Figure 4). The smartphone is employed here as an analyzer for accurate read out of the digitized information of the samples in a photograph instead of via the naked eye given the limited ability of the naked eye to distinguish between colors. There are some reported apps which can analyze the RGB value for captured photographs.[23,24] Here, the iPhone 12 with ColorColl app was employed as an example for the portable rapid pH analysis. Step 1, established an RGB standard reference pH chart: load the ColorColl app, then capture a photograph for each pH solution, directly click the target photograph, and readout the RGB value for each pH photograph to draw the standard pH chart. In order to obtain exact results, every pH sample was analyzed ten times. Step 2, rapidly analyze the unknown extreme pH sample: conduct similar operations to the samples above, and readout the RGB value for the tested sample, compare with the RGB standard reference pH chart, and output the test result immediately. Precise color signals were obtained through the successful utilization of the smartphone-integrated CDs sensing platform and a portable, precise, rapid, visual pH measurement device was realized.

Construction of a molecular "traffic signal". It should be noted that this color change process is reversible. The reversible fluorescence response under the acid-base conditions can be readily repeated for more than 10 cycles (Figure 5a). Given the reversible color changes and the presence of the "Green" "Brown" "Red" three color system, this can be viewed as being analogous to a traffic light. A simple but efficient logic circuit for the molecular traffic signal could be constructed (Figure 5b).[25] For the first input, a pH = 1 CDs **1** solution gives a pink emission, which can be designed as a red signal, and controls the traffic stop. The solution can be recycled and reused by adjustment of the pH to pH = 2 which gives a brown yellow emission, which controls the traffic to wait. Finally, the above solution can be further adjusted to pH 3, which would produce a green emission signal to direct the traffic to move.

Application in information encryption. Counterfeiting is increasingly a global problem that widely affects consumers, businesses and governments and leads to enormous financial loss and health risks. Anti-counterfeiting using information encryption by cheap, easily and stable fluorescent materials to protect high-value merchandise, documents and banknotes, and this is highly desirable.[26] With this in mind, the unique pH-induced color change phenomenon is exactly satisfied in the application of data encryption and decryption. As a proof-of-concept demonstration, CDs **1** inks can be written using a fountain pen. As shown in Figure S12, the encryption word "CHINA" is filled with CDs **1** ink, which is completely indiscriminate with any others under daylight. It only visibly fluoresces under UV irradiation. Owing to the excellent stability of CDs **1**, an obvious fluorescence was exhibited even after being stored indoors for several months. This simple encryption is convenient. Interestingly, this visible green fluorescence can be further turned to a pink color by spraying with HCl solution. The green fluorescence and pink fluorescence will be switched depending on the presence of the HCl. Inspired by this unique phenomenon, a secondary information encryption technology was further developed (Figure 5c). All of the letters written by our previously reported green fluorescent ink[27] except the confidential information "CHINA" was filled with CDs **1** ink. No matter if in daylight or under UV irradiation, they are completely indiscriminate from any others. The confidential information "CHINA" only appeared when it was sprayed with HCl and disappeared by simply heating the paper to remove the volatile HCl. This reversible fluorescence signal switching process enabled CDs **1** to provide enhanced security for anti-counterfeiting and realized the "Burn after reading" technology.

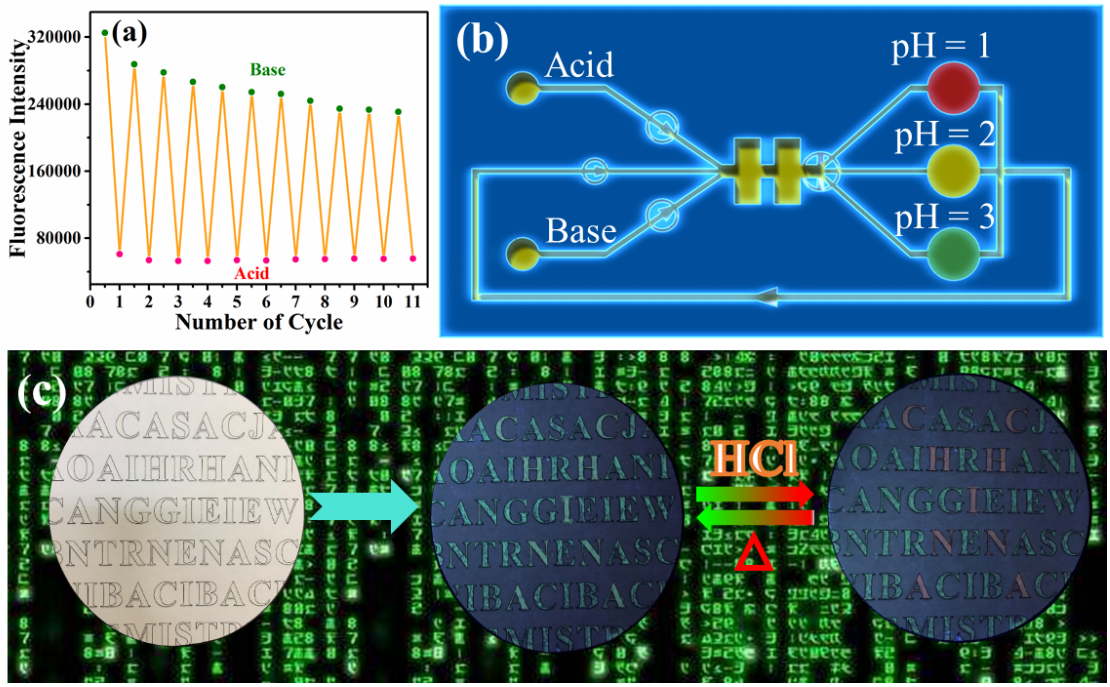

Figure 5. (a) The reversible fluorescence response curve of CDs **1** over 10 consecutive acid–base cycles (emission at 514 nm); (b) The schematic of molecular traffic signal light; (c) Photographs (under 365 nm UV light) and schematic illustration of secondary information encryption using CDs **1** with volatile HCl solution.

CONCLUTION

In conclusion, we have demonstrated that the photoluminescence properties of CDs can be tuned by simply modifying the functional groups of the carbon source. The obtained CDs **1** exhibited a unique pH-responsive behavior: it is very sensitivity toward both extreme acidity and basicity, but very stable under mild pH conditions (pH 4 to pH 11). In other words, CDs **1** can be employed as a pH nanosensor for use under extreme pH conditions, or as a stable biosensor over the wide mild pH range (pH 4 to pH 11). Under extremely acidic conditions (pH **1** to pH 3), the ratiometric change of CDs **1**'s fluorescence upon increasing of the pH resulted in a colorful change which enable us to monitor the pH change by naked eye. The naked eye detection resolution is up to 0.2 pH units which is higher than that for commercial precise pH test strips. Furthermore, a smartphone was employed in a portable precision pH measurement method, which eliminated the possible error from the naked eye. Inspired by the reversible color change on tuning the pH and the red/brown/green tri-emission fluorescence which corresponding to the pH 1/2/3, a molecular "signal traffic light" has been designed. Given the unique pH dependent photoluminescence properties, the CDs were further applied in the anti-counterfeiting and information encryption field and the "Burn after reading" encrypt technology was realized.

ASSOCIATED CONTENT

Supporting Information.

Experimental section, synthetic procedures, additional discussion, characterization and spectral data (PDF). This material is available free of charge via the Internet at http://pubs.acs.org.

AUTHOR INFORMATION

Corresponding Authors

* E-mail: zw.jin@siat.ac.cn (Z. Jin);
liucui@xjtu.edu.cn (C. Liu).

Notes

The authors declare no competing financial interest.

ACKNOWLEDGMENT

Dr. J.-L. Zhao thanks the Basic Research Program of Shenzhen (JCYJ20190812151405298) and the Shenzhen Peacock Plan support; Dr. C. Liu thanks the National Natural Science Foundation of China (21805021), China Postdoctoral Science Foundation (2020M683449, 2018M631057) and the Natural Science Foundation of Shaanxi province (2021JQ-009); Dr. Q. Luo thanks the Technology Program of Shenzhen (KCXFZ202002011008124); CR thanks the EPSRC for an Overseas Travel grant (EP/R023816/1).

REFERENCES

(1) a) Hou, J.-T.; Ren, W.-X.; Li, K.; Seo, J.; Sharma, A.; Yu, X.-Q.; Kim, J. S. Fluorescent bioimaging of pH: from design to applications. *Chem. Soc. Rev.* **2017**, 8, 2076-2090; b) Chen, Y. Recent advances in fluorescent probes for extracellular pH detection and imaging. *Anal. Biochem.* **2021**, 612, 113900; c) Chen, W.; Ma, X.; Chen, H.; Liu, S.; Yin, J. Fluorescent probes for pH and alkali metal ions. *Coord. Chem. Rev.* **2021**, 427, 213584.

(2) Schulthess, C. P. Historical perspective on the tools that helped shape soil chemistry. *Soil Sci. Soc. Am. J.* **2011**, 75, 2009-2036.

(3) a) Ding, L.; Li, X.; Hu, L.; Zhang, Y.; Jiang, Y.; Mao, Z.; Xu, H.; Wang, B.; Feng, X.; Sui, X. A naked-eye detection polyvinyl alcohol/cellulose-based pH sensor for intelligent packaging. *Carbohyd. Polym.* **2020**, 233, 115859; b) Bigdeli, A.; Ghasemi, F.; Abbasi-Moayed, S.; Shahrajabian, M.; Fahimi-Kashani, N.; Jafarinejad, S.; Nejad, M. A. F.; Hormozi-Nezhad, M. R. Ratiometric fluorescent nanoprobes for visual detection: Design principles and recent advances - A review. *Anal. Chim. Acta* **2019**, 1079, 30-58.

(4) Yue, Y.; Huo, F.; Lee, S.; Yin, C.; Yoon, J. A review: the trend of progress about pH probes in cell application in recent years. *Analyst* **2017**, 142, 30-41.

(5) a) Guo, Z.; Jiao, Y.; Du, F.; Gao, Y.; Lu, W.; Shuang, S.; Dong, C.; Wang, Y. Facile synthesis of ratiometric fluorescent carbon dots for pH visual sensing and cellular imaging. *Talanta* **2020**, 216, 120943; b) Niu, W.; Fan, L.; Nan, M.; Li, Z.; Lu, D.; Wong, M. S.; Shuang, S.; Dong, C. Ratiometric Emission Fluorescent pH Probe for Imaging of Living Cells in Extreme Acidity. *Anal. Chem.* **2015**, 87, 2788-2793; c) Yang, M.; Song, Y.; Zhang, M.; Lin, S.; Hao, Z.; Liang, Y.; Zhang, D.; Chen, P. R. Converting a Solvatochromic Fluorophore into a Protein-Based pH Indicator for Extreme Acidity. *Angew. Chem. Int. Ed.* **2012**, 51, 7674-7679.

(6) Yang, G.; Wan, X.; Su, Y.; Zeng, X.; Tang, J. Acidophilic S-doped carbon quantum dots derived from cellulose fibers and their fluorescence sensing performance for metal ions in an extremely strong acid environment. *J. Mater. Chem. A* **2016**, 4, 12841-12849.

(7) a) Martinsen, T. C.; Bergh, K.; Waldum, H. L. Gastric Juice: A Barrier Against Infectious Diseases. *Basic Clin. Pharmacol. Toxicol.* **2005**, 96, 94-102; b) Chao, D.; Chen, J.; Dong, Q.; Wu, W.; Qi, D.; Dong, S. Ultrastable and ultrasensitive pH-switchable carbon dots with high quantum yield for water quality identification, glucose detection, and two starch-based solid-state fluorescence materials. *Nano Res.* **2020**, 13, 3012-3018.

(8) Agrawal, A. M. Acid rain and its ecological consequences. *J. Environ. Biol.* **2008**, 29, 15-24.

(9) a) Krulwich, T. A.; Sachs, G.; Padan, E. Molecular aspects of bacterial pH sensing and homeostasis. *Nat. Rev. Microbiol.* **2011**, 9, 330-343; b) Foster, J. W. Escherichia coli acid resistance: tales of an amateur acidophile. *Nat. Rev. Microbiol.* **2004**, 2, 898-907; c) Merrell, D. S.; Camilli, A. Acid tolerance of gastrointestinal pathogens. *Curr. Opin. Microbiol.* **2002**, 5, 51-55.

(10) a) Qu, D.; Sun, Z. The formation mechanism and fluorophores of carbon dots synthesized via a bottom-up route. *Mater. Chem. Front.* **2020**, 4, 400-420; b) Dolai, S.; Bhunia, S. K.; Rajendran, S.; UshaVipinachandran, V.; Ray, S. C.; Kluson, P. Tunable fluorescent carbon dots: synthesis progress, fluorescence origin, selective and sensitive volatile organic compounds detection. *Crit. Rev. Solid State Mater. Sci.* **2020**, 1-22; c) Liu, M. L.; Chen, B. B.; Li, C. M.; Huang, C. Z. Carbon dots: synthesis, formation mechanism, fluorescence origin and sensing applications. *Green Chem.* **2019**, 21, 449-471; d) Silvi, S.; Credi, A. Luminescent sensors based on quantum dot–molecule conjugates. *Chem. Soc. Rev.* **2015**, 44, 4275-4289; e) Lim, S. Y.; Shen, W.; Gao, Z. Carbon quantum dots and their applications. *Chem. Soc. Rev.* **2015**, 44, 362-381.

(11) Xu, X.; Ray, R.; Gu, Y.; Ploehn, H. J.; Gearheart, L.; Raker, K.; Scrivens, W. A. Electrophoretic analysis and purification of fluorescent single-walled carbon nanotube fragments. *J. Am. Chem. Soc.* **2004**, 126, 12736-12737.

(12) a) Yan, Y.; Gong, J.; Chen, J.; Zeng, Z.; Huang, W.; Pu, K.; Liu, J.; Chen, P. Recent Advances on Graphene Quantum Dots: From Chemistry and Physics to Applications. *Adv. Mater.* **2019**, 31, 1808283; b) Yang, X. X.; Guo, Y. Z.; Liang, S.; Hou, S. Y.; Chu, T. T.; Ma, J. L.; Chen, X. H.; Zhou, J. H.; Sun, R. C. Preparation of sulfur-doped carbon quantum dots from lignin as a sensor to detect Sudan I in an acidic environment. *J. Mater. Chem. B*, **2020**, 8, 10788-10796; c) Wang, C.; Xu, J.; Li, H.; Zhao, W. Tunable multicolour S/N co-doped carbon quantum dots synthesized from waste foam and application to detection of Cr^{3+} ions. *Luminescence*, **2020**, 35, 1373-1383; d) Li, J. P.; Yang, S. W.; Liu, Z. Y.; Wang, G.; He, P.; Wei, W.; Yang, M. Y.; Deng, Y.; Gu, P.; Xie, X. M.; Kang, Z. H.; Ding, G. Q.; Zhou, H. F.; Fan, X. Q. Imaging Cellular Aerobic Glycolysis using Carbon Dots for Early Warning of Tumorigenesis. *Adv. Mater.* **2020**, 33, 2005096; e) Hu, C.; Dai, L. Doping of Carbon Materials for Metal-Free Electrocatalysis. *Adv. Mater.* **2019**, 31, 1804672.

(13) Jiang, K.; Sun, S.; Zhang, L.; Lu, Y.; Wu, A.; Cai, C.; Lin, H. Red, Green, and Blue Luminescence by Carbon Dots: Full-Color Emission Tuning and Multicolor Cellular Imaging. *Angew. Chem. Int. Ed.* **2015**, 54, 5360-5363.

(14) Geng, X.; Sun, Y.; Li, Z.; Yang, R.; Zhao, Y.; Guo, Y.; Xu, J.; Li, F.; Wang, Y.; Lu, S.; Qu, L. Retrosynthesis of Tunable Fluorescent Carbon Dots for Precise Long-Term Mitochondrial Tracking. *Small* **2019**, 15, 1901517.

(15) Zhao, J. L.; Wu, C.; Tomiyasu, H.; Zeng, X.; Elsegood, M. R.; Redshaw, C.; Yamato, T. A Rare and Exclusive Endoperoxide Photoproduct Derived from a Thiacalix[4]arene Crown-Shaped Derivative Bearing a 9,10-Substituted Anthracene Moiety. *Chem. Asian J.* **2016**, 11, 1606-1612.

(16) a) Lei, C.-W.; Hsieh, M.-L.; Liu, W.-R. A facile approach to synthesize carbon quantum dots with pH-dependent properties. *Dyes Pigments* **2019**, 169, 73-80; b) Yuan, F.; Ding, L.; Li, Y.; Li, X.; Fan, L.; Zhou, S.; Fang, D.; Yang, S. Multicolor fluorescent graphene quantum dots colorimetrically responsive to all-pH and a wide temperature range. *Nanoscale* **2015**, 7, 11727-11733; c) Pyne, A.; Layek, S.; Patra, A.; Sarkar, N. An easy and smart way to explore the light-emitting responses of carbon dot and doxorubicin hydrochloride assembly: white light generation and pH-dependent reversible photoswitching. *J. Mater. Chem. C* **2019**, 7, 6414-6425.

(17) Zhang, H.; Liu, S. Mixing concentrated sulfuric acid and diethylenetriamine at room temperature: A rapid and facile approach to synthesize fluorescent carbon polymer hollow spheres as peroxidase mimics. *J. Colloid Interface Sci.* **2021**, 582, 405-411.

(18) a) Hu, Y.; Yang, Z.; Lu, X.; Guo, J.; Cheng, R.; Zhu, L.; Wang, C.-F.; Chen, S. Facile synthesis of red dual-emissive carbon dots for ratiometric fluorescence sensing and cellular imaging. *Nanoscale* **2020**, 12, 5494-5500; b) Wang, Q.; Yang, H. T.; Zhang, Q.; Ge, H. G.; Zhang, S. R.; Wang, Z. Y.; Ji, X. H. Strong acid-assisted preparation of green-emissive carbon dots for fluorometric imaging of pH variation in living cells. *Microchim. Acta* **2019**, 186, 468.

(19) a) Liu, C.; Bao, L.; Yang, M.; Zhang, S.; Zhou, M.; Tang, B.; Wang, B.; Liu, Y.; Zhang, Z.-L.; Zhang, B.; Pang, D.-W. Surface Sensitive Photoluminescence of Carbon Nanodots: Coupling between the Carbonyl Group and π-Electron System. *J. Phys. Chem. Lett.* **2019**, 10, 3621-3629; b) Bao, L.; Liu, C.; Zhang, Z.-L.; Pang, D.-W. Photoluminescence-Tunable Carbon Nanodots: Surface-State Energy-Gap Tuning. *Adv. Mater.* **2015**, 27, 1663-1667; c) Hu, Y.; Gao, Z. Hot-injection strategy for 1-min synthesis of carbon dots from oxygen-containing organic solvents: Toward fluorescence sensing of hemoglobin. *Dyes Pigments* **2019**, 165, 429-435.

(20) a) Wu, S.; Min, H.; Shi, W.; Cheng, P. Multicenter Metal–Organic Framework-Based Ratiometric Fluorescent

Sensors. *Adv. Mater.* **2019**, 32, 1805871; b) Zhang, H.; Sun, T.; Ruan, Q.; Zhao, J.-L.; Mu, L.; Zeng, X.; Jin, Z.; Su, S.; Luo, Q.; Yan, Y.; Redshaw, C. A multifunctional tripodal fluorescent probe for the recognition of Cr^{3+}, Al^{3+}, Zn^{2+} and F^{-} with controllable ESIPT processes. *Dyes Pigments* **2019**, 162, 257-265.

(21) a) Choudhury, D. S.; Chethodil J. M.; Gharat P. M.; Praseetha, P. K.; Pal, H. pH-elicited luminescence functionalities of carbon dots: mechanistic insights. *J. Phys. Chem. Lett.* **2017**, 8, 1389-1395; b) Ye, X.; Xiang, Y.; Wang, Q.; Li, Z.; Liu, Z. A Red Emissive Two-Photon Fluorescence Probe Based on Carbon Dots for Intracellular pH Detection. *Small* **2019**, 15, 1901673; c) Yang, P.; Zhu, Z.; Zhang, T.; Zhang, W.; Chen, W.; Cao, Y.; Chen, M.; Zhou, X. Orange-Emissive Carbon Quantum Dots: Toward Application in Wound pH Monitoring Based on Colorimetric and Fluorescent Changing. *Small*, **2019**, 15, 1902823; d) Liu, C.; Yang, M.; Hu, J.; Bao, L.; Tang, B.; Wei, X.; Zhao, J.; Jin, Z.; Luo, Q.; Pang, D. W. Quantitatively Switchable pH-Sensitive Photoluminescence of Carbon Nanodots. *J. Phys. Chem. Lett.* **2021**, 12, 2727-2735.

(22) Valeur, B. *Molecualr Fluorescence: Principles and Application*, Wiley-VCH Verlag GmbH, Weinheim (Federal Republic of Germany) **2002**, 100-106.

(23) Wang, Y.; Zhang, P.; Fu, W.; Zhao, Y. Morphological control of nanoprobe for colorimetric antioxidant detection. *Biosens. Bioelectron.* **2018**, 122, 183-188.

(24) Fan, Y. Z.; Dong, J. X.; Zhang, Y.; Li, N.; Liu, S. G.; Geng, S.; Ling, Y.; Luo, H. Q.; Li, N. B. A smartphone-coalesced nanoprobe for high selective ammonia sensing based on the pH-responsive biomass carbon nanodots and headspace single drop microextraction. *Spectrochim. Acta Mol. Biomol. Spectros.* **2019**, 219, 382-390.

(25) Ni, X.-L.; Zeng, X.; Redshaw, C.; Yamato, T. Ratiometric fluorescent receptors for both Zn^{2+} and $H_2PO_4^{-}$ ions based on a pyrenyl-linked triazole-Modified homooxacalix[3]arene: A potential molecular traffic signal with an R-S latch logic circuit. *J. Org. Chem.* **2011**, 76, 5696-5702.

(26) a) Zhao, J.; Zheng, Y.; Pang, Y.; Chen, J.; Zhang, Z.; Xi, F.; Chen, P. Graphene quantum dots as full-color and stimulus responsive fluorescence ink for information encryption. *J. Colloid Interface Sci.* **2020**, 579, 307-314; b) Huang, W.; Xu, M.; Liu, J.; Wang, J.; Zhu, Y.; Liu, J.; Rong, H.; Zhang, J. Hydrophilic Doped Quantum Dots “Ink” and Their Inkjet-Printed Patterns for Dual Mode Anticounterfeiting by Reversible Cation Exchange Mechanism. *Adv. Funct. Mater.* **2019**, 29, 1808762; c) Ren, W.; Lin, G.; Clarke, C.; Zhou, J.; Jin, D. Optical Nanomaterials and Enabling Technologies for High-Security-Level Anticounterfeiting. *Adv. Mater.* **2019**, 32, 1901430.

(27) Fang, J.-A.; Zhao, J.-L.; Liao, X.; Zeng, X.; Chen, K.; Wei, X.-Y.; Su, S.-B.; Luo, Q.-Y.; Redshaw, C.; Jin, Z. Molecular Tweezers-like Calix[4]arene Based Alkaline Earth Metal Cation (Ca^{2+}, Sr^{2+}, and Ba^{2+}) Chemosensor and Its Imaging in Living Cells and Zebrafish. *Inorg. Chem.*, **2019**, 58, 14720-14727.

Table of Contents